



**HAL**  
open science

## Mechanical Properties of Adhesive Films Obtained from PU-Acrylic Hybrid Particles

Elise Degrandi-Contraires, Ravindra Udagama, Elodie Bourgeat-Lami,  
Timothy Mckenna, Keltoum Ouzineb, Costantino Creton

► **To cite this version:**

Elise Degrandi-Contraires, Ravindra Udagama, Elodie Bourgeat-Lami, Timothy Mckenna, Keltoum Ouzineb, et al.. Mechanical Properties of Adhesive Films Obtained from PU-Acrylic Hybrid Particles. *Macromolecules*, 2011, 44 (8), pp.2643-2652. 10.1021/ma2000702 . hal-00723734

**HAL Id: hal-00723734**

**<https://hal.science/hal-00723734>**

Submitted on 22 Dec 2021

**HAL** is a multi-disciplinary open access archive for the deposit and dissemination of scientific research documents, whether they are published or not. The documents may come from teaching and research institutions in France or abroad, or from public or private research centers.

L'archive ouverte pluridisciplinaire **HAL**, est destinée au dépôt et à la diffusion de documents scientifiques de niveau recherche, publiés ou non, émanant des établissements d'enseignement et de recherche français ou étrangers, des laboratoires publics ou privés.

**Mechanical Properties of adhesive films obtained from PU-acrylic hybrid particles**

Journal:	<i>Macromolecules</i>
Manuscript ID:	ma-2011-000702
Manuscript Type:	Article
Date Submitted by the Author:	12-Jan-2011
Complete List of Authors:	Creton, Costantino; E.S.P.C.I., Laboratoire PPMD-UMR 7615 Degrandi-Contraires, Elise; E.S.P.C.I., Laboratoire PPMD Bourgeat-Lami, Elodie; Laboratoire de Chimie et Procédés de Polymérisation, LCPP - CNRS - CPE McKenna, Timothy; CNRS-LCPP (Laboratory of Chemistry and Processes of Polymerization) Udagama, Ravindra; CNRS-LCPP (Laboratory of Chemistry and Processes of Polymerization) Ouzineb, Keltoum; Cytec Surface Specialties

SCHOLARONE™  
Manuscripts

Confidential - ACS

1  
2  
3  
4  
5  
6  
7  
8  
9  
10  
11  
12  
13  
14  
15  
16  
17  
18  
19  
20  
21  
22  
23  
24  
25  
26  
27  
28  
29  
30  
31  
32  
33  
34  
35  
36  
37  
38  
39  
40  
41  
42  
43  
44  
45  
46  
47  
48  
49  
50  
51  
52  
53  
54  
55  
56  
57  
58  
59  
60

**Part II: Mechanical Properties of adhesive films obtained from PU-acrylic  
hybrid particles**

Elise Degrandi-Contraires,<sup>1</sup> Ravindra Udagama,<sup>2</sup> Elodie Bourgeat-Lami,<sup>2</sup> Timothy McKenna,<sup>2</sup> Keltoum Ouzineb,<sup>3</sup> Costantino Creton<sup>1\*</sup>

<sup>1</sup>Laboratoire de Physico-Chimie des Polymères et Milieux Dispersés, CNRS-UPMC-ESPCI Paristech, 10 rue Vauquelin, 75231 Paris cedex 05, France

<sup>2</sup>Université de Lyon, Univ. Lyon 1, CPE Lyon, CNRS UMR 5265, Laboratoire de Chimie, Catalyse, Polymères et Procédés (C2P2), LCPP group, 43 Bd du 11 Novembre 1918, F-69616, Villeurbanne, France.

<sup>3</sup> Research and Technology, Cytec Surface Specialties, Anderlecht Street 33, 1620 Drogenbos, Belgium

**Abstract**

The mechanical and adhesive properties of films made from novel hybrid urethane/acrylic dispersions have been investigated. The adhesive films were obtained from the drying of bicomponent acrylic urethane latexes prepared by miniemulsion polymerization. Phase separation at the macroscopic scale was avoided by using a NCO end-functionalized polyurethane (PU) prepolymer and a hydroxy ethyl methacrylate (HEMA) reactive comonomer in the acrylic backbone<sup>1</sup>. The effect of two compositional parameters on the mechanical and adhesive properties was specifically studied: the PU weight fraction and the degree of grafting of the PU prepolymer on the acrylic backbone, controlled by the ratio between grafting agent HEMA and chain extender Bisphenol A (BPA). Swelling, rheological, tensile and probe-tack tests were used in parallel with an analysis of the macroscopic adhesive properties of the films. Results show that the PU weight fraction modifies significantly the small-strain elastic modulus and the gel fraction in the latex particle while the ratio HEMA/BPA can be used to adjust the chain length of the PU incorporated in the network. This ratio affects significantly the finite extensibility of the PSA while causing only relatively small changes in the low strain elastic modulus and gel fraction. An increase in the degree of grafting at fixed PU content is found to improve the resistance to shear of the adhesive without reducing its adhesion energy in a peel or probe tack test.

## Introduction

Pressure-sensitive adhesives (PSA) are soft polymeric materials displaying an instantaneous adhesion on most surfaces upon application of a light pressure. Although the function appears relatively simple, the design of proper PSA is complex and relies heavily either on polymer chemistry (for acrylic and silicone polymers) or on formulation (for block copolymers and natural rubbers) in order to obtain sparsely crosslinked polymer networks with optimized properties<sup>2-7</sup>. This optimization means that the PSA must be able to dissipate energy during the peeling process (a property optimized for a highly viscous entangled polymeric liquid) and must be resistant to creep in shear (optimum when some crosslinking is present preventing flow).

Acrylic PSA<sup>4, 8</sup> are generally weakly crosslinked copolymers of low  $T_g$  which have insoluble and soluble fractions, respectively called gel and sol. A very broad molar mass distribution (i.e. high polydispersity) of the sol fraction and a cohesive network formed by the gel is a good and relatively easy way to achieve a practical solution, but has limitations due to the impossibility of independently control the architecture of sol and gel during a simple synthesis. The fine control of the network structure of the gel becomes an essential aspect of advanced techniques to achieve a better balance of properties.

A possible design path to achieve a better control of the network structure is to incorporate another polymer (such as an alkyd or a polyurethane) to form hybrid materials. The preparation of these hybrid materials could potentially lead to a more favourable combination of properties compared with those of the initial purely acrylic PSA. Because of environmental concerns however, we have focused our study on emulsion-based acrylic PSA<sup>8</sup>. In emulsion-based systems, the independent control of the network structure of the gel and of the sol fraction is more difficult. Furthermore, the control of the interfaces between particles remaining after drying is problematic and can strongly affect the mechanical properties<sup>9, 10</sup>.

However, the development of miniemulsion polymerization<sup>11, 12</sup> has helped to overcome the main issue of the homogeneous incorporation of a hydrophobic polymer in a waterborne acrylic polymer. The advantage of miniemulsion polymerization is that it is possible to directly incorporate a hydrophobic polymer (e.g. PU) into the monomer droplets during the droplet formation step, and then directly polymerize the droplets to get a hybrid where the components are mixed on the scale of nanometers<sup>12</sup>. If these hydrophobic compounds contain

1  
2 reactive functional groups, such as unsaturated double bonds, then they can be chemically  
3 incorporated into the growing polymer chains during the free radical polymerization.  
4

5  
6 Many different components have been incorporated successfully into hybrid systems in this  
7 manner, and several reviews are available presenting the technique and the possibilities of  
8 hybridization<sup>11-14</sup>.  
9

10  
11 A number of studies have investigated the synthesis of acrylic-polyurethane (PU) systems.  
12 Successful incorporations have been reported by the formation of interpenetrating networks  
13<sup>15</sup>, by the formation of a core-shell structure<sup>16</sup> or by standard emulsion with a polyurethane  
14 dispersion as a seed<sup>17</sup>. In all cases, the transparency and homogeneity of the hybrid were  
15 better than those of the physical blends. However miniemulsion polymerization appears to be  
16 a versatile and powerful method to graft polyurethane to an acrylic polymer as exposed in the  
17 work of Udagama *et al.*<sup>1</sup>, of Wang *et al.*<sup>18-22</sup> or again of Li, El-Aasser and coworkers<sup>23</sup>. In the  
18 latter study, it is shown that the grafting prevents phase separation at the particle scale  
19 between polyurethane and acrylic copolymer. Most studies focused on applications as  
20 coatings, where advantages of combining acrylic with urethane for PSA applications are  
21 potentially numerous: better film-formation, better mechanical stability or temperature  
22 resistance<sup>23-25</sup> and where a precise control of the polymer architecture is not necessary since  
23 crosslinkers (dryers) are often added. To the best of our knowledge ours is the first study  
24 focusing on acrylic polymers for adhesive applications where the control of the polymer  
25 architecture is essential to obtain the desired properties and where a precise control of a low  
26 level of crosslinking<sup>26</sup> and of the entanglement structure is essential<sup>27</sup>.  
27  
28  
29  
30  
31  
32  
33  
34

35  
36 In this study and in its companion paper<sup>1</sup>, we selected a model acrylic copolymer typical of  
37 those used for PSA, and investigated the incorporation of a minority fraction of a low molar  
38 mass reactive PU in the acrylic particle. Part I<sup>1</sup> focuses on the synthesis methods while part II,  
39 the current paper, focuses on the effect of changing synthesis parameters on the adhesive  
40 properties and relates such changes to the network structure, characterized by mechanical tests  
41 on dry films and by swelling experiments.  
42  
43  
44  
45  
46  
47  
48  
49  
50  
51  
52

## Experimental

### Synthesis

All samples have been synthesized in batch via miniemulsion polymerization. The details of the polymerisation procedure are described in a companion paper<sup>1</sup> and we only briefly recall here the main synthesis parameters which are necessary to understand the results.

The monomer composition of the acrylic matrix was: butyl acrylate (BA, 89.5 wt%), methyl methacrylate (MMA, 9.5 wt%) and acrylic acid (AA, 1 wt%). A NCO terminated polyurethane (PU) prepolymer (Incorez 701, Industrial Copolymers Limited) was incorporated in the acrylic polymer particles. This incorporation was performed in three steps:

1) The PU prepolymer chains were dissolved in the organic monomer phase, which also contained the hydrophobic costabilizer: octadecyl acrylate (ODA). Hydroxy ethyl methacrylate (HEMA) was added and a known amount of NCO functions was reacted with a known amount of HEMA. We thus define the percentage of HEMA to NCO (% HEMA to NCO). This step was conducted for 12 hours at 25°C using dibutyltin dilaurate as catalyst and results in the grafting of NCO to the HEMA.

2) A known amount of Bisphenol A (BPA) was added to the organic phase containing PU and the dibutyltin dilaurate catalyst and reacted for 30 minutes at 25°C. The role of this BPA was to extend the PU chains and complete the reaction with the remaining NCO groups.

3) The organic phase containing the monomers and the HEMA-functionalized BPA-extended PU chains were added to the aqueous solution containing surfactant (Dowfax 2A1). Nanodroplets were formed by ultrasonication. The radical polymerization was initiated with the addition of a redox initiator pair (Tertiary Butyl HydroPeroxide, TBHP, and Sodium Formaldehyde Sulfoxylate, SFS) and miniemulsion polymerization was carried out at 50°C.

1-Dodecyl mercaptan was used as a chain transfer agent (CTA) to control the kinetic chain length and therefore gel formation. 0.2 wt% with respect to monomers was added unless mentioned otherwise. It is important to note that butyl acrylate is much more prone than methylmethacrylate to chain transfer during free radical polymerization and naturally leads to branched architectures of the polymer in the absence of CTA, ODA was used as hydrophobic component and was added to the particles to avoid Ostwald ripening. Three

series of samples were prepared. In the first series, the molar ratio between OH and NCO functions was equal to 0.55 and the molar ratio of OH functions from the HEMA to OH functions from the BPA (the HEMA/BPA ratio) was kept equal to 0.22. The polyurethane weight fraction was changed from 5 wt% to 50 wt% based on monomers. In the second series, a fixed quantity of PU (25 wt%) was incorporated in the particles. The ratio OH/NCO was fixed at 0.55 and the ratio HEMA/BPA was changed from 0.11 to 0.50. In the last series, ODA was excluded from the synthesis and the ratio OH/NCO was increased to 1. Two samples with 25 wt% of PU were prepared with different HEMA/BPA (respectively 0.10 and 0.25) and different CTA contents (respectively 0.3 and 0.2). Finally, one blank latex with no PU, no HEMA and no BPA was prepared with a CTA content of 0.2%. Table 1 summarizes the important formulation parameters for the different samples.

Table 1. Description of the different series of latexes

Lab code	CTA <sup>a</sup>	PU <sup>b</sup>	HEMA (mol% to NCO)	OH/NCO	HEMA/BPA <sup>b</sup>
T150	0.2	5	10	0.55	0.22
T151		15			
T152		35			
T153		50			
T147		25	5		0.11
T145			10		0.22
T148			15		0.36
T149	20		0.50		
T160	0.3	25	10	1	0.10
T161	0.2		20	0.25	
T170	0.2	0	/	/	/

<sup>a</sup>Wt% relative to monomers. <sup>b</sup>Molar ratio of the OH groups from HEMA to the OH group from BPA.

### Polymer characterization

The solid content of the latexes was measured gravimetrically and was ~ 50 wt% of polymer for all latexes.

6

1  
2 We measured the gel content and the swelling ratio,  $Q$ , by static measurements. A small piece  
3 of solid film was cut and weighed ( $W_1$ ) and was then immersed in THF for a week. After a  
4 week, the sample which was completely swollen by the solvent was taken out and weighed  
5 again ( $W_2$ ). It was then dried at 60 °C for 30 minutes to extract all the solvent and the dried  
6 sample was weighed ( $W_3$ ).  
7  
8

9  
10  
11 The gel content was given by:  $\%gel = \frac{W_3}{W_1} \times 100$  (1)  
12

13  
14 And the swelling ratio by:  $Q = \frac{W_2}{W_3}$  (2)  
15  
16

17  
18 The glass transition temperature of the final polymer samples ( $T_g$ ) was measured by  
19 Differential Scanning Calorimetry (DSC; TA Instrument DSC 2920). Two cycles were  
20 performed at cooling and heating rates of 10 °C.min<sup>-1</sup>. The  $T_g$  was obtained from the second  
21 cycle.  
22  
23

#### 24 25 26 **Mechanical characterization**

27  
28  
29 Samples for the rheological and tensile experiments were prepared as follows: a given volume  
30 of latex was deposited in silicone moulds and dried at room temperature for one week. The  
31 moulds were covered with a bell-jar to protect them from dust. The volume of latex was  
32 calculated to give the required final film thickness depending on the latex solid content. After  
33 a week, the moulds were held for 5 minutes at 110°C. The samples were then removed,  
34 placed between low-release silicone papers and cut to the desired dimensions with a die-  
35 cutter.  
36  
37

38  
39  
40 For the probe-tack experiments, the latexes were deposited on microscope glass-slides also  
41 protected from dust by a bell-jar, and dried 48 hours at room temperature. They were finally  
42 dried for 1 minute at 110°C and the resulting films, with an average thickness of 120µm, were  
43 kept in plastic boxes before use. All samples were used within a week of preparation.  
44  
45

46  
47 The linear viscoelastic properties of the adhesives were characterized with a rheometer RDAII  
48 using parallel plate geometry. Frequency sweeps (0.3-120 rad.s<sup>-1</sup>) with an applied strain  
49  
50

1  
2 between 5% and 10% were made on 500  $\mu\text{m}$  thick samples of 8 mm as diameter at room  
3 temperature.  
4

5  
6 To analyze the large-strain behaviour, we used a standard tensile INSTRON machine (model  
7 5565) equipped with a videoextensometer (model SVE). The machine uses a 10 N load cell  
8 with a resolution of  $\pm 1$  mN. Rectangular strips of 5 mm wide ( $w_0$ ) with an average thickness  
9 ( $e_0$ ) of the order of 500 $\mu\text{m}$  were cut within the self-standing films. Individual values were  
10 controlled for each sample. The initial velocity of the crosshead was chosen to obtain an  
11 initial strain rate of  $1 \text{ s}^{-1}$  which is roughly equivalent to the initial strain rate applied during  
12 the adhesion tests and all tests were performed at room temperature. The force-displacement  
13 curve obtained is then converted to nominal stress  $\sigma_N = F/A_0$  vs. stretch  $\lambda = l/l_0$   
14  
15  
16  
17

18  
19 The adhesive properties were characterized with two types of tests: a laboratory probe test<sup>28, 29</sup>  
20 and a series of standard industrial tests. In the probe tack test, a stainless steel probe comes in  
21 contact with the adhesive layer deposited on a glass slide. After a set contact time, the probe  
22 is withdrawn at a constant velocity. A mirror is installed upon the glass slide and allows the  
23 visualisation of the debonding mechanism and the measurement of the real contact area for  
24 each sample. We used standard parameters for the temperature (Room Temperature),  
25 approach velocity ( $V_{\text{app}} = 30 \mu\text{m}\cdot\text{s}^{-1}$ ), contact time ( $t_c = 1 \text{ s}$ ) and contact force ( $F_c = -70 \text{ N}$ ).  
26 The debonding rate was varied between 1 and 1000  $\mu\text{m}/\text{s}$  but we report here only data for the  
27 debonding velocity ( $V_{\text{deb}} = 100 \mu\text{m}\cdot\text{s}^{-1}$ ) for the purpose of comparing materials. The force was  
28 measured by a load cell (250N, resolution 0.5 N). The displacement of the probe was  
29 measured with an LVDT extensometer (range 5mm, resolution 0.5 $\mu\text{m}$ ). The force and  
30 displacement for each curve were normalized by the contact area of the probe (as visualized  
31 with the camera) and by the initial thickness of the film to obtain a stress vs. strain curve  
32 which will be used to compare adhesive films.  
33  
34  
35  
36  
37  
38  
39  
40

41 The characterization of the adhesive properties of the films with industrial standard tests  
42 (FINAT) was carried out as follows. The latexes were dried on a polyester (PE) backing film  
43 during 3 minutes at 110  $^\circ\text{C}$  to obtain dry adhesive film thicknesses of 23 $\mu\text{m}$  which are  
44 standard in industry. These adhesive + PE layers were then bonded to a stainless steel (SS)  
45 substrate.  
46  
47  
48

49 The shear resistance was defined by measuring the holding time (in minutes) before failure of  
50 a 1 inch<sup>2</sup> adhesive layer to which a mass of 1 kg was applied (FINAT test method 8). The  
51  
52

53  
54  
55  
56  
57  
58  
59  
60

1  
2 maximum time measured was 10000 min. After this limiting time, the test was stopped. If a  
3 cohesive failure occurred, CF was noted along with the value of the holding time at failure. It  
4 is worth noting that for a commercial PSA, cohesive failure is neither desirable in the case of  
5 the shear resistance test nor in the case of the probe test.  
6  
7

## 8 9 10 **Results and discussion**

11  
12 Before discussing the specific effects of the PU weight fraction and of the degree of grafting,  
13 it is useful to briefly summarize the DSC results. The PU has no apparent effect on the heat  
14 capacity scans and a single  $T_g$  of  $-39 \pm 3$  °C is detected for all hybrid adhesive films. For  
15 comparison, the  $T_g$  of the pure PU is estimated to be around  $-48$  °C. Therefore, the large  
16 distribution of the  $T_g$  of the copolymer and its proximity with the  $T_g$  of the PU could mask a  
17 possible phase separation.  
18  
19  
20  
21  
22

### 23 24 25 **1. Role of the PU weight fraction**

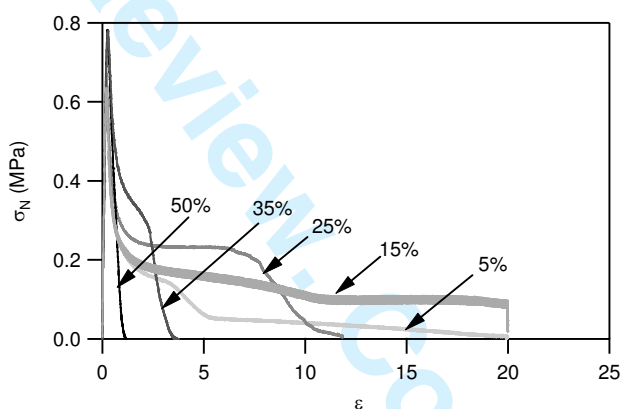
#### 26 27 **1.1. Adhesive properties**

28  
29 In the first series of samples (sample T150 to T153 in table 1), the effect of the weight  
30 fraction of reactive PU incorporated in the polymer was investigated. Figure 1 presents probe-  
31 tack results for this series. The relevant parameters chosen to analyse these results were the  
32 plateau stress at intermediate and larger strain and the maximum strain. The plateau stress  $\sigma_f$   
33 is related to fibrillation observed during the debonding, while the maximum strain  $\epsilon_{max}$   
34 corresponds to the final detachment from the probe<sup>28</sup>. Figure 1 shows that samples with a low  
35 amount of polyurethane (less than 25% based on the total amount of acrylic monomers) are  
36 characterized by a low fibrillation stress and a high maximum strain  $\epsilon_{max}$ <sup>a</sup>. The residues  
37  
38  
39  
40  
41  
42  
43  
44

---

45  
46 <sup>a</sup> For 15wt% of PU, the stress does not go back to zero for technical reasons. The maximum scale of the  
47 extensometer measuring the probe displacement is 5 mm. For the 15% sample, when the probe reaches 5 mm,  
48 fibrils joining the probe and the adhesive layer remain. These fibrils neither fail for a high deformation nor after  
49 waiting a long time. They can break cohesively or adhesively when the test is stopped and the probe is removed  
50 manually.  
51  
52

1  
2 remaining on the probe after the test indicate a cohesive debonding inside the fibrils. These  
3 tack curves are characteristic of samples with a low level of elasticity, due to a low level of  
4 crosslinking. On the other hand, for samples with 35 wt% or 50 wt% of PU, the tack curves  
5 show almost no fibrillation plateau and the  $\epsilon_{\max}$  is low. Despite nucleation of cavities at the  
6 onset of debonding, these cavities coalesce and interfacial propagation of cracks leads to an  
7 interfacial debonding<sup>30,31</sup>. Finally, the sample with 25% of PU forms a fibrillar structure upon  
8 debonding, and debonds at a maximum strain  $\epsilon_{\max}$  of the order of 10 which is typical of many  
9 commercial PSA's. The final drop of the stress is characteristic of adhesive debonding, and  
10 results in the absence of residues on the probe. Thus, adhesive properties are best for this  
11 fraction of PU.  
12  
13  
14  
15  
16  
17  
18  
19  
20  
21  
22  
23  
24  
25  
26  
27  
28  
29  
30  
31  
32



33 Figure 1. Stress-strain tack curves for the 5 PU weight fractions with 0.2% CTA and  
34 HEMA/BPA=0.22;  $V_{\text{deb}}=100 \mu\text{m}\cdot\text{s}^{-1}$  (i.e.  $d\epsilon/dt=1 \text{ s}^{-1}$ )  
35  
36  
37  
38

39 Table 2. Adhesion energy measured for  $V_{\text{deb}}=100 \mu\text{m}\cdot\text{s}^{-1}$  and industrial shear resistance results  
40

Sample name	PU (wt%)	Gel fraction (%)	$W_{\text{adh}}$ ( $\text{J}\cdot\text{m}^{-2}$ ) <sup>a</sup>	Shear resistance (min)
T170	0	47.3	$200.4 \pm 21.2$	$181 \pm 15$ CF
T150	5	Not measurable	$161.4 \pm 43.2$ CF	$46 \pm 15$ CF
T151	15	25.7	$379.3 \pm 111.3$ CF	$222 \pm 15$ CF
T145	25	37.4	$284.9 \pm 93.3$	$9463 \pm 15$ CF
T152	35	57.9	$143.62 \pm 39.9$	Not measured
T153	50	73.8	$49.6 \pm 5.2$	> 10000

51  
52  
53  
54  
55  
56  
57  
58  
59  
60

<sup>a</sup> For  $V_{deb}=100 \mu\text{m}\cdot\text{s}^{-1}$ . <sup>b</sup> At  $300\text{mm}\cdot\text{min}^{-1}$

Table 2 presents results from probe-tack tests, gel measurements and industrial shear tests. The comparison between probe test results, which measure the energy dissipated during fast debonding, and shear resistance, which is a measure of the resistance to failure at long times illustrates the difficulty in finding an optimum. Clearly the samples with 5 and 15% of PU are still dissipative but shear resistance is not much improved relative to the standard acrylic. The sample with 50% PU has an exceptional resistance to shear but does not dissipate much energy upon debonding. In the end the best compromise in properties appears to be the sample with 25% PU which combines an improvement in tack and a 50 fold increase in shear resistance. The most interesting result here is the comparison of the best hybrid PSA (T145) with the pure acrylic matrix (T170) showing that both adhesion energy and resistance to shear have been improved by the incorporation of the PU in the material.

The interpretation of these results requires a finer characterization of the differences in the network structure.

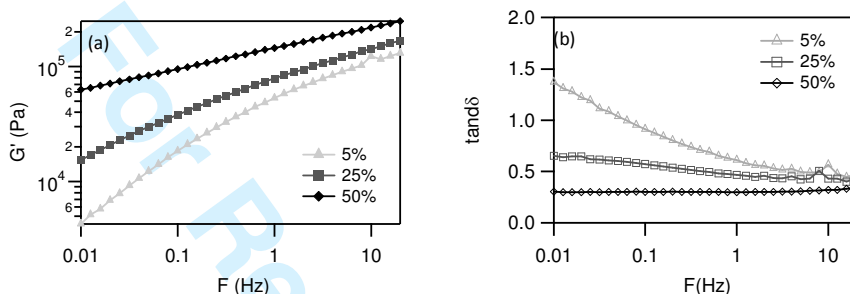
This characterization was carried out with the help of three different methods which are complementary: Rheological measurements reveal the level of viscoelasticity, large strain tensile experiments are a sensitive probe of the finite extensibility of the network chains and of the dissipation of energy taking place at large strains and the swelling and gel fraction measurements inform on the architecture of the polymer.

### 1.2. *Linear viscoelasticity*

Since decades the linear viscoelastic properties of pressure-sensitive-adhesives have been considered the best predictor of the adhesive properties<sup>32-35</sup>. From fully empirical criteria, we have now moved to more mechanistically based semi-empirical criteria which are able to predict to a certain extent the performance of PSA<sup>30</sup>.

Figure 2 shows the variation of the storage modulus and  $\tan\delta$  with frequency, for three adhesive films with increasing PU content. At equivalent degree of grafting, the more PU is added to the hybrid, the higher is its elastic modulus and the lower is  $\tan\delta$ . It is clear that the dissipation becomes much lower and frequency-independent in the presence of high PU contents. This shows that the number of pendant chains and free chains decreases

1  
2 significantly with PU content. It also suggests that the entanglement density (at high  
3 frequency at room temperature) increases with PU content.  
4  
5  
6  
7



8  
9  
10  
11  
12  
13  
14  
15  
16  
17  
18  
19  
20  
21 Figure 2. Evolution of  $G'$  (a) and  $\tan\delta$  (b) as a function of frequency for different PU weight  
22 fractions: 5 wt% (T150), 25 wt% (T145) and 50 wt% (T153).  $T = 25^\circ\text{C}$   
23  
24

25 These linear viscoelastic properties can be used to predict the suitability of the soft network  
26 for PSA applications. The value of the storage modulus at 1 Hz should be below 100 kPa  
27 to allow an easy contact with a rough surface<sup>36</sup>. The value of  $\tan\delta/G'$  at the relevant debonding  
28 frequency can be used as a finer criterion to predict whether fibrillation will occur or not upon  
29 debonding<sup>30, 37, 38</sup>. For the sample with 50% of PU, the value of  $G'$  is  $1.45 \cdot 10^5$  Pa, i.e. in the  
30 upper limit to conform to the surface. At the tack test frequency (1 Hz), the value of  $\tan\delta/G'$  is  
31  $0.21 \cdot 10^{-5} \text{ Pa}^{-1}$ , which is inferior to the lower limit of  $0.5 \cdot 10^{-5} \text{ Pa}^{-1}$  reported to be required to  
32 have fibrillation debonding on steel<sup>30, 39</sup>. The fact that  $\tan\delta/G'$  is too low indicates a lack of  
33 dissipation coupled to a high value of the elastic modulus, completely consistent with the  
34 observed interfacial debonding.  
35  
36  
37  
38  
39

40 Conversely, for 5% of PU, the storage modulus meets Dahlquist criterion ( $0.53 \cdot 10^5$  Pa) and  
41 the level of dissipation is very high. As a result the debonding criteria is very high ( $\tan\delta/G' \sim$   
42  $1.15 \cdot 10^{-5} \text{ Pa}^{-1}$  at 1 Hz). Dissipation dominates and we are in presence of a highly deformable  
43 material which readily forms fibrils upon debonding. This is again consistent with the  
44 cohesive failure observed in adhesion tests.  
45  
46  
47

48 As observed with the tack test, the value of 25 wt% of PU in the latex represents an optimum  
49 value for the viscoelastic properties as well. Indeed, both the stiffness and the fibrillation  
50  
51  
52

53 12  
54  
55  
56  
57  
58  
59  
60

1  
2 (tan $\delta$ /G') criteria are fulfilled with G'(1Hz) equal to 0.99 10<sup>5</sup> Pa and tan $\delta$ /G' equal to 0.6 10<sup>-5</sup>  
3 Pa<sup>-1</sup> at 1Hz, and fibrillation debonding is indeed observed.  
4

5  
6 The differences in viscoelastic behaviour reflect differences in the architecture of the polymer  
7 inside the particle. Table 2 gives the gel fraction in the adhesive film for the five PU contents.  
8 For 5% PU, the gel fraction is too low to be measured. Then it increases to 70-80% for the  
9 high PU-content samples.  
10

11  
12 The characterization of the gel fraction is a good indicator of the viscoelastic behaviour. The  
13 partially crosslinked gel imparts elasticity while the pendant chains attached to the gel and the  
14 sol fraction control the time dependent stress relaxation. Based on the differences in linear  
15 viscoelastic properties and gel fraction, the incorporation of PU at fixed grafting ratio  
16 increases the crosslink density, the entanglement density (high frequency G') and decreases  
17 the density of pendant chains and the soluble fraction..  
18  
19  
20  
21

### 22 23 24 **1.3. Large strain behaviour**

25  
26 While linear rheology experiments are useful to predict whether fibrils will form or not after  
27 the initial cavitation stage, the final detachment of these fibrils can only be predicted through  
28 the analysis of the large strain behaviour<sup>40-42</sup>. Figure 3 shows the results of tensile  
29 experiments for the five samples with different amounts of PU. Very significant differences  
30 due to the presence of PU are immediately apparent not only in the absolute values of the  
31 stress at equivalent strain but in the overall shape of the stress strain curve. The two samples  
32 with the lowest PU weight fractions (T150 and T151) do not present any hardening at large  
33 strain but simply flow at a nearly constant nominal stress.  
34  
35  
36  
37  
38  
39  
40  
41  
42  
43  
44  
45  
46  
47  
48  
49  
50  
51  
52  
53  
54  
55  
56  
57  
58  
59  
60

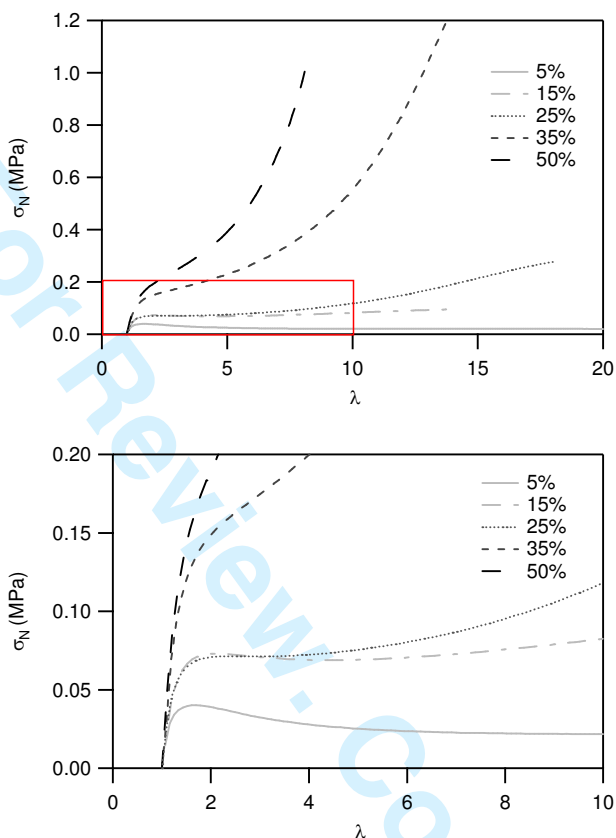


Figure 3. Nominal stress versus lambda for the 5 different PU weight fractions;  $d\varepsilon/dt=1s^{-1}$ ; the bottom figure is a magnification of the red square

As it is obvious from looking at the curves of Figure 3, the tensile behaviour of these weakly crosslinked networks is highly non linear, and shows a pronounced relaxation or softening after about  $\lambda = 1.5$ . For almost all PSA's this softening is both strain and strain rate dependent and curves measured at a single strain rate can be fitted equally well by a viscoelastic model<sup>26</sup> or by a nonlinear elastic model<sup>43</sup>. However if tensile tests are carried out at two different strain rates with the same material, it is impossible to fit both curves with the same material parameters with either model. A quantitative modelling of the large strain behavior of a PSA would require a full fledged non-linear viscoelastic model including finite extensibility. Such

1  
2 a model has not yet been developed. However it is possible to use a simpler and approximate  
3 methodology to characterize the PSA behaviour in large strain.  
4

5  
6 First the Young's modulus  $E_y$  can be measured at small strains. It is defined as the slope of a  
7 line fitting the curve between  $\lambda=1$  and  $\lambda=1.02$ . This quantity represents the unrelaxed  
8 modulus and should be directly comparable with  $G'(\omega)$  at the appropriate strain rate.  
9

10  
11 Second, the deviation of the stress-strain curve relative to the prediction from Gaussian rubber  
12 elasticity can be analyzed from the Mooney representation. The reduced stress  $\sigma_R$ , also named  
13 Mooney stress, is defined as:  
14

$$\sigma_R = \frac{\sigma_N}{\left(\lambda - \frac{1}{\lambda^2}\right)}$$

15  
16  
17  
18  
19  
20  
21 It corresponds to the nominal stress normalized by  $\left(\lambda - \frac{1}{\lambda^2}\right)$ . For a Neo-Hookean rubber, the  
22 reduced stress is constant as a function of  $\lambda$  and is simply equal to the shear modulus  $G$ . For a  
23 PSA, this reduced stress is not constant and is typically represented as a function of the  
24 inverse of strain  $1/\lambda$ <sup>30</sup>. Two characteristic parameters of the non-linear behaviour can be  
25 determined: the  $C_{\text{soft}}$  to characterize the softening at intermediate strain and the  $C_{\text{hard}}$   
26 characterizing the onset of strain hardening at large strain<sup>30</sup>.  $C_{\text{soft}}$  is defined as the slope of a  
27 line drawn between  $(\sigma_R(0.8); 1/\lambda = 0.8)$  and  $(\sigma_{R\text{min}}; 1/\lambda_{\text{min}})$ .  $C_{\text{hard}}$  is defined as the reduced  
28 stress corresponding to the minimum in  $\sigma_R$ . Another interesting parameter is  $\lambda_{\text{hard}}$ , i.e. the  
29 strain level corresponding to the minimum reduced stress and hence to the onset of strain  
30 hardening. Strain hardening or more accurately strain stiffening<sup>44</sup> is correlated to the finite  
31 extensibility of the chains and thus to the network architecture. The ratio  $C_{\text{soft}}/C_{\text{hard}}$   
32 characterizes, in large strain the balance between relaxing and non-relaxing crosslink points  
33 and should be optimized for a PSA<sup>6, 30</sup>.  
34  
35  
36  
37  
38  
39  
40  
41

42 The Mooney representations as a function of PU content are shown in Figure 4 while Table 3  
43 gives the values of the viscoelastic parameters  $C_{\text{soft}}$  and  $C_{\text{hard}}$ , the ratio  $C_{\text{soft}}/C_{\text{hard}}$  and the  
44 Young's modulus.  
45  
46  
47  
48  
49  
50  
51  
52  
53  
54  
55  
56  
57  
58  
59  
60

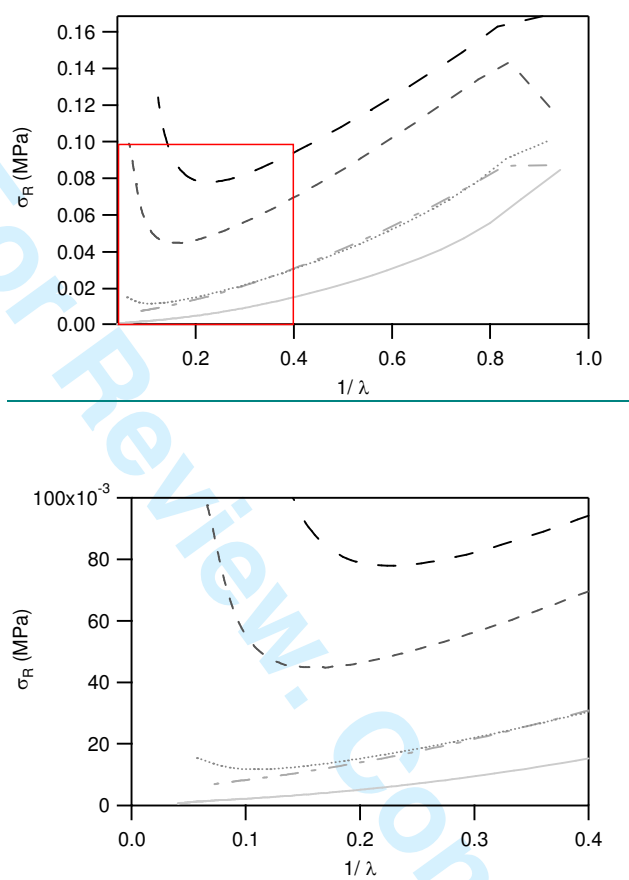


Fig.4: Reduced stress versus inverted lambda for the 5 different PU weight fractions;  $d\epsilon/dt=1s^{-1}$ ; the bottom figure is a magnification of the region in the red square

Table 3. Values of the Mooney-Rivlin viscoelastic parameters for different PU amounts;  $d\epsilon/dt=1s^{-1}$

Sample Code	PU (wt%)	$C_{soft}$ (kPa)	$C_{hard}$ (kPa)	$C_{soft}/C_{hard}$	E (kPa)
T150	5	84.5	No min in $\sigma_R$	$\infty$	141.4
T151	15	115.9	No min in $\sigma_R$	$\infty$	239.7
T145	25	109.4	11.8	9.3	275.6
T152	35	147.3	44.8	3.2	329.6

T153	50	143.6	77.9	1.8	459.9
------	----	-------	------	-----	-------

The ratio  $C_{\text{soft}}/C_{\text{hard}}$  reflects the balance between the extent of relaxation at intermediate strain and hardening at large strain. It decreases significantly with increasing PU content, reflecting the less and less viscoelastic character of the films (see Figure 5). The Young's modulus is a small-strain high frequency modulus. It is affected by both chemical crosslinks and entanglements (that are all trapped at high frequencies). However in a fully acrylic matrix it is usually not much affected by a low level of crosslinking<sup>26, 43</sup>. Its increase with PU content indicates that the network has clearly more entanglements with increasing PU. The increase of  $C_{\text{hard}}$  on the other hand only reflects the increase in chemical crosslinks. The non measurable density of such crosslinks for 5 wt% and 15 wt% of PU is fully consistent with the observed cohesive failure of these two adhesives in the tack experiments. The absence of strain stiffening at large strains prevents the fibrils from detaching from the surface without leaving residues. The T145 and T153 samples have values of  $C_{\text{hard}}$  and  $C_{\text{soft}}$  in the range of classic purely acrylic PSA's. The values of  $C_{\text{hard}}$  reflecting also the density of permanent crosslinks can be cross-checked also by a measurement of the swelling capacity of the gel fraction of the polymer.

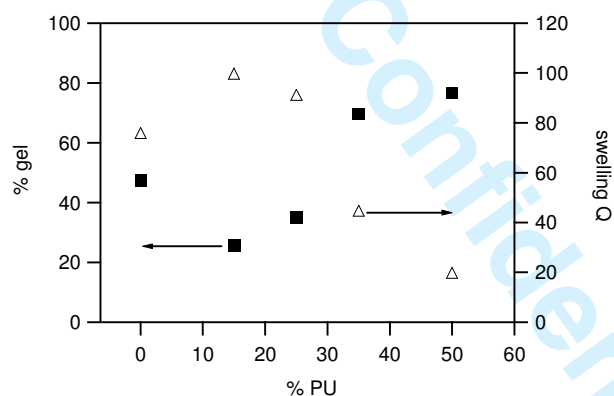


Figure 5. Evolution of the gel fraction (■) and of the swelling ratio (Δ) with the polyurethane content

Figure 5 shows the change in gel fraction and equilibrium swelling of the gel as a function of PU content. The sharp increase in gel fraction with PU content is consistent with the viscoelastic measurements: the addition of PU reduces the uncrosslinked fraction and limits

1  
2 relaxation from free chains and pendant chains. It also dramatically changes the equilibrium  
3 swelling of the gel which means that the density of elastically active chains (attached at both  
4 ends) in the gel increases significantly. Finally if the equilibrium swelling is compared in  
5 Figure 6 with the hardening strain  $\lambda_{\text{hard}}$  obtained from tensile experiments of the films.  $\lambda_{\text{hard}}$   
6 decreases with the equilibrium swelling  $Q$ , which indicates that the PU chains considerably  
7 shorten the average length of the acrylic chains between crosslink points. This is due to the  
8 fact that, at fixed stoichiometry, more PU means more HEMA and hence more grafting  
9 points. Therefore the average molecular weight between grafting points on the acrylic chains  
10 decreases.  
11  
12  
13  
14  
15  
16  
17  
18  
19  
20  
21  
22  
23  
24  
25  
26  
27  
28  
29  
30  
31  
32  
33  
34  
35  
36  
37  
38  
39  
40  
41  
42  
43  
44  
45  
46  
47  
48  
49  
50  
51  
52  
53  
54  
55  
56  
57  
58  
59  
60

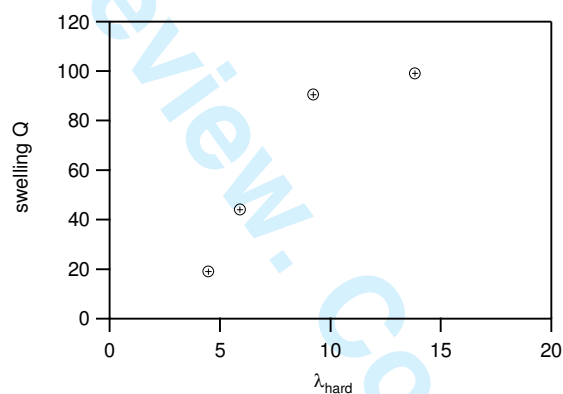


Figure 6. Evolution of the swelling  $Q$  with the hardening strain  $\lambda_{\text{hard}}$

### Summary

These combined results indicate that the network becomes much more densely crosslinked when the PU weight fraction increases. However it is interesting to note that a small amount of PU actually reduces the gel fraction and the strain stiffening, relative to a purely acrylic matrix. This reduction in crosslinking is probably due to a reduction in the acrylic kinetic chain length since the bisphenol-A favors chain transfer<sup>45,46</sup>.

The gel fraction and swelling experiments confirm that the NCO-terminated PU enhances crosslinking of the PU polymer chains to the acrylic network through the HEMA. In essence the PU would appear to act like any low molecular weight crosslinker.

1  
2 Yet this is misleading because, in addition, PU chains are also more densely entangled than  
3 the acrylic chains because of the PPG constituting their soft segment ( $M_e \sim 3 - 5 \text{ kg.mol}^{-1}$  for  
4 the PU<sup>47</sup> while  $M_e \sim 20 - 30 \text{ kg.mol}^{-1}$  for the acrylics<sup>48</sup>). Thus, the PU adds both chemical and  
5 physical crosslinks and this is the reason for the significant increase in the small-strain  
6 modulus. The very significant softening observed for all PU hybrids would be very difficult to  
7 obtain with a purely acrylic network.  
8

9  
10  
11 The consequence on adhesive properties of this continuous variation in crosslinking and  
12 entanglement density with PU content is a clear transition from under-crosslinked to over-  
13 crosslinked materials. Only one of the adhesives gives a network architecture adapted to a  
14 PSA application and a reasonable balance between relaxation and hardening. This sample  
15 debonds adhesively in a fibrillation mode, with relatively high adhesion energy. An  
16 equivalent optimum in the PU weight fraction has been observed by Wang *et al.*<sup>20</sup> in the  
17 same type of PU/acrylic hybrid prepared for coating applications.  
18  
19  
20  
21  
22

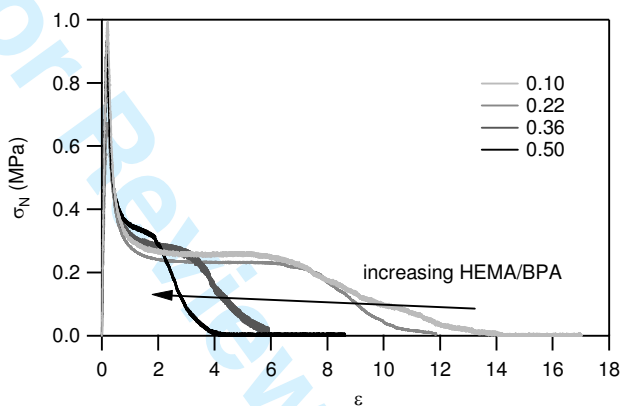
## 24 2. Impact of the degree of grafting of the PU

25  
26  
27 If the PU content is fixed, the second parameter that can be varied is the level of grafting of  
28 the PU chains to the acrylic matrix. The reaction between HEMA and NCO-terminated PU  
29 can be well controlled during the synthesis<sup>1</sup>. In the following series, the fraction of NCO  
30 actually consumed during HEMA grafting is varied from 5 to 20mol%, taking into account  
31 that 20% is the maximum level of grafting allowed by the reaction between HEMA and PU<sup>1</sup>.  
32 For a fixed total amount of OH groups, the degree of grafting is directly connected to the  
33 HEMA/BPA molar ratio. In this section, we compare samples with a constant weight fraction  
34 of PU (25%) and HEMA/BPA ratios changing from 0.1 to 0.5 with a ratio between OH and  
35 NCO fixed at 0.55.  
36  
37  
38  
39  
40  
41  
42

### 43 2.1. Adhesive properties

44  
45 Figure 7 shows the probe tack curves obtained for different degrees of grafting at a PU  
46 content of 25% and a CTA amount of 0.2%. For these synthesis conditions, a fibrillation  
47 plateau is always observed but cohesive failure of fibrils is sometimes observed for the  
48 sample with HEMA/BPA=0.10. The maximum deformation  $\epsilon_{\text{max}}$  of the adhesive layer  
49  
50  
51  
52

1  
2 decreases markedly when the ratio HEMA/BPA increases. A lower  $\epsilon_{\max}$  means that fibrils are  
3 less stretched at detachment and this is due to a combination of more strain stiffening and  
4 probably less dissipation near the interface<sup>40</sup>. Conversely, the fibrillation stress  $\sigma_f$  of the tack  
5 curves increases with HEMA/BPA.  
6  
7



8  
9  
10  
11  
12  
13  
14  
15  
16  
17  
18  
19  
20  
21  
22  
23  
24  
25  
26  
27 Figure 7. Stress-strain tack curves for 4 different HEMA/BPA ratios;  $V_{\text{deb}}=100 \mu\text{m}\cdot\text{s}^{-1}$  (i.e.  
28  $d\epsilon/dt = 1 \text{ s}^{-1}$ )  
29

30  
31  
32 Table 4 compares quantitatively the adhesion energy obtained with the probe-tack test at  $V_{\text{deb}}$   
33  $= 100 \mu\text{m}\cdot\text{s}^{-1}$  to the results of the shear resistance tests for different HEMA/BPA ratios. The  
34 low grafting regime is particularly interesting. While increasing the adhesion energy relative  
35 to the pure acrylic matrix, the resistance to shear increases dramatically. Similar to the effect  
36 of PU content it is now interesting to examine the effect of the HEMA/BPA ratio on the  
37 network architecture.  
38  
39  
40  
41

42  
43 Table 4. Adhesion energy measured at  $V_{\text{deb}} = 100 \mu\text{m}\cdot\text{s}^{-1}$  and industrial shear and peel results  
44 for the blank sample and the 4 HEMA/BPA ratios; in all cases  $\text{OH}/\text{NCO}=0.55$ .  
45

Sample name	HEMA/BPA	$W_{\text{adh}}$ ( $\text{J}\cdot\text{m}^{-2}$ )	Shear resistance (min)
T170	0.0	$200.4 \pm 21.2$	$181 \pm 15$ CF
T147	0.11	$548.4 \pm 128.2$	$1680 \pm 15$ CF

46  
47  
48  
49  
50  
51  
52  
53  
54  
55  
56  
57  
58  
59  
60  
20

T145	0.22	$284.9 \pm 93.3$	$9463 \pm 15CF$
T148	0.36	$164.6 \pm 21.3$	> 10000

## 2.2. Linear viscoelastic properties

$G'$  and  $\tan\delta$  as a function of frequency for different HEMA/BPA ratios with 25 wt% of PU are shown in figure 8. Above 1 Hz, both change little with the ratio HEMA/BPA and are in the acceptable range for PSA applications. The resulting values of  $\tan\delta/G'$  are all predicting a fibrillation debonding (from  $0.44 \cdot 10^5 \text{ Pa}\cdot\text{s}^{-1}$  for the lower HEMA/BPA (T147) to  $0.40 \cdot 10^5 \text{ Pa}\cdot\text{s}^{-1}$  for the higher ratio (T149)). In conclusion changes of the grafting ratio at fixed PU content do not greatly affect the linear viscoelastic properties.

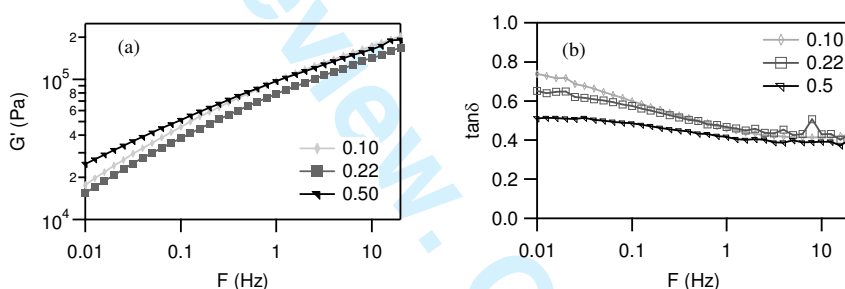


Figure 8. Evolution of the  $G'$  (a) and of the ratio  $\tan\delta/G'$  (b) as a function of frequency for HEMA/BPA=0.10 (T147), for HEMA/BPA=0.22 (T145) and for HEMA/BPA=0.50 (T149);  $\varepsilon \sim 8\%$ .

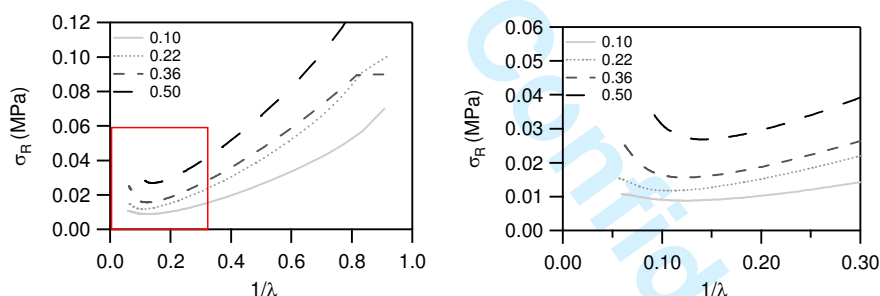
This relative insensitivity of the linear viscoelastic properties with grafting ratio are confirmed by the gel fraction measurements which all show a gel fraction varying between 36 and 54 % and increasing slightly with increasing HEMA/BPA ratio.

## 2.3. Large strain experiments

The tensile experiments are more sensitive to the subtle changes in polymer architecture and they have been performed on the same samples at a nominal strain rate  $d\varepsilon/dt=1\text{s}^{-1}$ . To emphasize these fine changes, we choose here the Mooney representation, as explained in 1.3 (Figure 9). The different curves have a similar shape for all the HEMA/BPA ratios. The main

1  
2 difference is in the onset of strain hardening, as can be seen on the magnified curve (fig. 9-  
3 right). From the Mooney plot, one can observe that  $C_{\text{soft}}$  and  $\lambda_{\text{hard}}$  do not change much but  
4  $C_{\text{hard}}$  does. The increase of  $C_{\text{hard}}$  shows that HEMA/BPA mostly affects the density of  
5 permanent crosslinks, i.e. the bridges created by the PU chains, but not the finite extensibility  
6 of the network presumably controlled by the longer chains of the acrylic network. Such an  
7 apparently conflicting result can only be obtained with a heterogeneously crosslinked  
8 network, i.e. some densely crosslinked zones (which swell less and provide stiffness) and  
9 some less crosslinked zones which percolate and can extend. The values of  $C_{\text{soft}}$  (Table 5)  
10 remain relatively constant except for the lowest grafting density where the relaxation is very  
11 fast and as a consequence the value of  $C_{\text{soft}}/C_{\text{hard}}$  decreases with grafting density. This  
12 decrease in viscoelastic character combined with the increased level of strain stiffening causes  
13 the differences in adhesion energy that are observed.

20  
21 Measurements of the gel fraction (relatively constant for HEMA/BPA between 0.1 and 0.36)  
22 confirm this scenario: equilibrium swelling from  $Q = 85$  at low grafting to  $Q = 55$  at high  
23 grafting. Finally because the PU fraction is fixed the density of entanglements is also fixed  
24 and the small strain modulus slightly changes.



40 Figure 9. Reduced stress versus  $1/\lambda$  for the 4 different HEMA/BPA ratios;  $d\varepsilon/dt=1\text{ s}^{-1}$ ; the  
41 bottom figure is a magnification of the red square.

42  
43 Table 5. Values of the Mooney-Rivlin viscoelastic parameters for the 4 different HEMA/BPA  
44 ratios;  $d\varepsilon/dt=1\text{ s}^{-1}$

45  
46  
47  
48

Sample name	HEMA/BPA	$C_{\text{soft}}$ (kPa)	$C_{\text{hard}}$ (kPa)	$C_{\text{soft}}/C_{\text{hard}}$	$E_y$ (kPa)
T147	0.11	67.9	8.9	7.7	191.5
T145	0.22	109.4	11.8	9.3	275.6

49  
50  
51

52  
53 22  
54  
55  
56  
57  
58  
59  
60

T148	0.36	106.5	15.65	6.8	244.7
T149	0.50	116.2	26.9	4.3	414.9

### Summary

The crosslinked network architecture is modified by the HEMA/BPA ratio but differently than by the PU content. Decreasing the HEMA/BPA ratio is equivalent to decreasing the density of PU bridges incorporated in the network. However this time this change occurs mostly in the gel fraction and does not greatly affect the finite extensibility of the network probably because of a heterogeneous gel structure. As a result, the adhesion energy remains relatively constant but the material can be made a little less crosslinked (favourable for adhesion on low energy surfaces) or more crosslinked (favourable for high shear resistance).

One can conclude that at fixed 25% PU content, the change in grafting ratio affects the crosslinking density of more crosslinked domains in a heterogeneous gel structure and does not affect much the sol fraction. It affects the low frequency dissipation in the polymer network, improving the resistance to flow, and not the small strain and high frequency elasticity. It is then possible to use separate synthetic tools to adjust the storage modulus (PU fraction) and the finite extensibility (PU grafting).

### 3. Effect of the OH/NCO ratio

As described in a companion paper, during the miniemulsion synthesis, it is necessary to add a hydrophobic monomer to avoid Ostwald ripening of particles<sup>12</sup>. Here 5.15 % in weight (relative to the monomer content) of octadecylacrylate (ODA) was incorporated in the recipe. In presence of this hydrophobic component, it was not possible to incorporate the total amount of BPA required to give a stoichiometric ratio  $\text{OH/NCO} = 1$ . For amounts higher than 50% of the theoretical amount, flocculation of the particles was observed during the synthesis<sup>1</sup>.

The consequence for the polymer architecture and mechanical properties is that the PU chains are expected to be less extended by BPA. Furthermore, as no isocyanate can be observed by

$^{13}\text{C}$  NMR, it is reasonable to assume that reaction with water occurs. In other words, the reaction of polyurethane prepolymer chains is not completely controlled.

To promote a total reaction of the remaining isocyanate with BPA, some samples have been prepared without costabilizer ODA and with  $\text{OH}/\text{NCO}=1$ . No flocculation was observed and some solid films have been prepared from these new latexes to evaluate the impact of the  $\text{OH}/\text{NCO}$  ratio on the mechanical properties and the polymer architecture. In these samples, 25 wt% of PU is incorporated and two grafting ratios of the PU were chosen: 20% (high grafting) and 10% (low grafting). CTA content also varied from 0.2% for the high grafting to 0.3% for the low grafting (see Table 1). Probe-tack and tensile results of four samples are presented in figure 10.

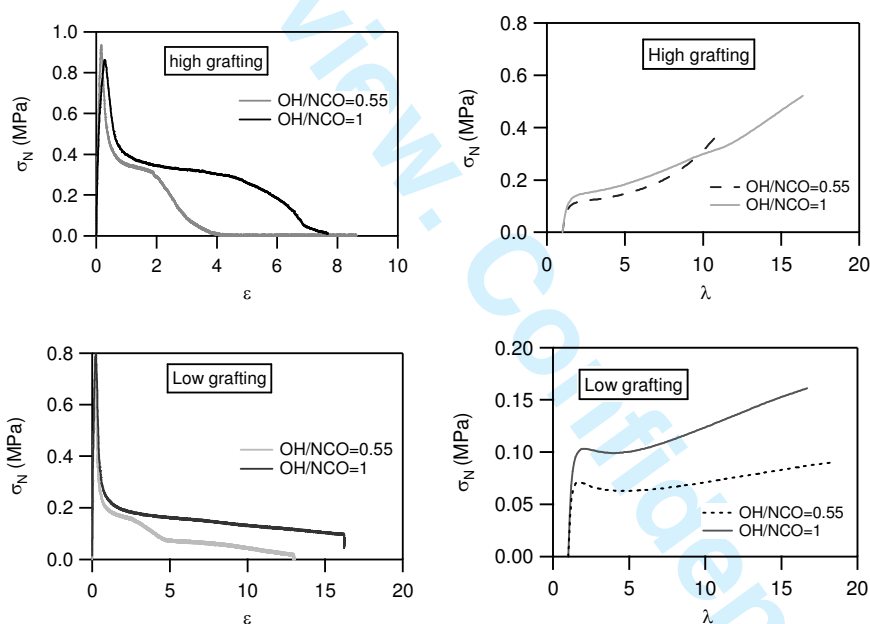


Figure 10. Probe tack (left) and tensile results (right) of samples with  $\text{OH}/\text{NCO}=0.55$  and  $\text{OH}/\text{NCO}=1$  for high grafting of PU (top; samples T149 and T161) and low one (down; samples T147 and T160); for probe-tack tests  $V_{\text{deb}}=100\mu\text{m}\cdot\text{s}^{-1}$  (i.e.  $d\epsilon/dt=1\text{s}^{-1}$ ); for tensile tests  $d\epsilon/dt=1\text{s}^{-1}$

As seen in Figure 10, the effect of the change in process is different in the case of high grafting level and low grafting level. Nevertheless, in both cases, the increase in the amount

1  
2 of BPA has a positive effect. For high grafting the deformability of the sample is significantly  
3 improved. When a high degree of grafting of PU is used, the material synthesized with more  
4 BPA has a higher maximum extension before debonding while maintaining the level of  
5 plateau stress. Based on the previous conclusions, it is consistent with constant grafting and  
6 constant PU fraction. The tensile curves show a less pronounced softening for the sample with  
7 high BPA amount and a more progressive hardening at very large strains. The polymer  
8 network is more deformable with equivalent small-strain stiffness. Our hypothesis is that the  
9 presence of BPA may act there as a chain transfer and reduce the kinetic chain length of the  
10 acrylic, effectively making the hybrid network a bit more viscoelastic and extensible. This  
11 confirms the hypothesis of longer acrylic chains formed with the presence of a higher amount  
12 of BPA and thus higher deformability. The gel and swelling measurements partially confirm  
13 this interpretation. The gel content decreases from 54.5 % for OH/NCO=0.55 (less BPA) to  
14 44.3 % for OH/NCO=1 (more BPA). On the other hand, the swelling increases from 57.0  
15 (less BPA) to 74.6 (more BPA). Considering the extraction technique used to measure the gel  
16 content, values may appear closed but their trend is consistent with the other observations.  
17 Indeed, they indicate that the network is less crosslinked, but with only a small effect of the  
18 decrease in the gel fraction on the elasticity.

19  
20 For low grafting, probe-tack tests show a longer plateau, due to a stabilized fibrillation  
21 process. In tensile experiments the softening takes place at a higher stress and hardening is  
22 more pronounced. These observations reflect that the material is less deformable with more  
23 BPA. In this case, it may be argued that the extension of PU chains by BPA can help to  
24 connect dangling chains together to create PU bridges and increase the gel content and thus  
25 the stiffness. Unfortunately, the extraction and swelling measurements could not be done due  
26 to the low level of crosslinking in the samples.

27  
28 If the effect of the extension on the mechanical properties (see Figure 11) is clear in both  
29 cases, it is not easy to locate the transition from the first mechanism (reduction of acrylic  
30 chain length) to the second one (formation of new PU bridges) and the effect of reaction with  
31 water is also unclear.

32  
33 On the point of view of the application as PSA, the best results in tack, peel and shear are  
34 obtained for hybrid latexes with 25% of polyurethane compared to the acrylic monomers,  
35 with OH/NCO=1, HEMA/BPA ~ 0.25 and 0.2% CTA.

#### 4. General discussion: Network structure of the urethane/acrylic hybrids

Several molecular analysis have demonstrated three ideas<sup>1</sup>. First, all NCO groups have reacted with HEMA, BPA or water. Then, SEC analysis and inverse titration have shown that the molar mass of the PU prepolymer is  $\sim 3000 \text{ g.mol}^{-1}$ , and finally it is known that only a maximum of 20mol% of NCO groups can react with HEMA. Therefore, PU chains can be incorporated in three different ways:

- BPA-extended chains which have reacted on both side with HEMA form bonded PU chains. After acrylic polymerization, these chains will be part of the gel fraction.
- BPA-extended chains which have reacted on only one side with HEMA are dangling chains. They are terminated either by a BPA or by an amine (obtained after reaction with water). These chains are connected to the acrylic backbone at only one side.
- BPA-extended chains which did not react with any HEMA are called free chains. They are part of the soluble fraction inside the particles.

These three types of chains coexist in the particles and their proportions and lengths obviously change according to the fraction of PU, the ratio OH/NCO and the ratio HEMA/BPA.

To have an appropriate representation of the architecture of the hybrid network inside particles, one has to take in account two other important parameters. The molar mass of the acrylic copolymers ( $300\text{--}4000 \text{ kg.mol}^{-1}$  depending on the samples) is much higher than that of the PU, even extended. Then, assuming that the soft chain is mostly polyether (polypropylene glycol PPG), the PU chains are much more entangled than the acrylic ones.  $M_e$  for this type of PU has been found to be around  $3\text{--}5 \text{ kg.mol}^{-1}$ <sup>47</sup> when it is  $\sim 20\text{--}30 \text{ kg.mol}^{-1}$  for the main monomer, butyl acrylate<sup>48,49</sup>

Taking in account the different connections of the PU chains, a schematic representation of the network is presented in Figure 11 (except that no reaction of NCO with water is shown).



Figure 11: Theoretical urethane/acrylic hybrid network

The presence of PU affects not only the viscoelastic balance but also the finite extensibility of the adhesive layer by connecting the acrylic backbones. As discussed above, even significantly extended PU grafted chains remain shorter than the acrylic chains. Moreover, most of the chains are bonded chains connected to the acrylic at both ends. In this context the onset of strain stiffening is controlled by the length of the acrylic chains between two grafting points. The change in mechanical properties as a function of grafting density suggest that the PU may not be distributed homogeneously in each particle, with some PU rich zones connected together by PU poor zones.

Two important caveats need to be mentioned here. First no reaction with water is considered in this description. In reality, some of the NCO functions will react with water during the miniemulsification process and the early stages of the synthesis reaction<sup>1, 23, 50</sup>. This fraction may modify the architecture of the polymer.

Second, in all the discussions above, we have ignored the particle morphology and assumed implicitly a homogeneous incorporation of the PU. This is consistent with the appearance of the films which are clear, transparent and crack-free at least at macroscopic level. This is also in good agreement with the unique  $T_g$  measured by DSC. Nevertheless, the arguments above plead for the existence of heterogeneous structures and a phase separation occurring at the particle scale for 25 wt% of PU and a degree of grafting of 10 % cannot be ruled out. The possible existence of these nanodomains which are more crosslinked but are embedded in a

1  
2 less crosslinked matrix polymer, seem to have little effect on the dissipation of energy during  
3 debonding but to greatly strengthen the resistance to shear of the material. This would also be  
4 consistent with a recently published study on nanostructured adhesives<sup>51</sup>  
5  
6  
7

## 8 9 10 **Conclusion**

11 The key findings of our study can be summarized as follows:

12  
13 The amount of polyurethane (at fixed OH/NCO ratio) affected strongly the ratio between  
14 soluble and insoluble parts because of the addition of crosslinking points between the NCO-  
15 terminated PU chains and the acrylic chains. Moreover, since the polyurethane is more  
16 entangled than the acrylic, it also affected the small strain elastic modulus with the  
17 incorporation of many entanglements, which behave like permanent crosslinks at high  
18 frequency but can relax at low frequency or high temperature.  
19

20  
21 The degree of grafting at fixed PU content (controlled by the ratio between the grafting agent  
22 HEMA and the chain extender BPA) plays an important role in the architecture of the  
23 insoluble part. The analysis of the tensile tests strongly suggest a heterogeneous particle  
24 structure with a minority of more crosslinked PU rich domains and a majority of less  
25 crosslinked and percolating PU-poor domains.  
26

27  
28 As a result of this heterogeneous structure, industrial standard tests on the adhesive properties  
29 of the PSA have shown a clear improvement in shear resistance while the adhesion energy  
30 remained acceptable for standard applications. This clearly showed that the detailed structure  
31 of the gel part of the PSA is as important as the gel fraction itself, a point which has been  
32 often neglected so far.  
33

34  
35 Clearly, the fine control of the polymer structure inside a particle with a bicomponent system  
36 remains very challenging. Several reactions compete kinetically and the final result is likely to  
37 depend on the details of the procedure and on the details of the composition such as amount  
38 of chain transfer agent used, nature of the initiator, and of course temperature of the reaction.  
39 Furthermore the materials studied here have been produced with a batch process relatively far  
40 from the conditions used in industrial applications.  
41

42  
43 Nevertheless the general trends discovered should be broadly applicable to the design of  
44 hybrid networks containing both polycondensation reactions and free radical polymerization.  
45 All previous publications on urethane/acrylic networks focused on high  $T_g$  coatings which  
46 have much less propensity to chain transfer reactions and are more sensitive to the details of  
47  
48  
49  
50  
51

52  
53 28  
54  
55  
56  
57  
58  
59  
60

1  
2 the interfaces between particles<sup>19, 20, 23</sup>. To our knowledge this is the first study on the design  
3 of such a network in soft adhesives.  
4  
5  
6  
7

## 8 Acknowledgments

9  
10 The EU Framework 6 Integrated Project NAPOLEON NMP3-CT-2005-01184 is  
11 acknowledged for the financial support provided to this project.  
12  
13

## 14 References

- 15 1. Udagama, R.; Graillat, C.; Degrandi-Contraires, E.; Creton, C.; Bourgeat-Lami, E.;  
16 McKenna, T. *submitted*.
- 17 2. Tobing, S. D.; Klein, A. *Journal of Applied Polymer Science* **2001**, *79*, 2558-2564.
- 18 3. Tobing, S. D.; Klein, A. *Journal of Applied Polymer Science* **2001**, *79*, 2230-2244.
- 19 4. Satas, D., Acrylic Adhesives. In *Handbook of pressure-sensitive-adhesives*, 2nd ed.;  
20 Satas, D., Ed. Van Nostrand Reinhold: New York, 1989; Vol. 1, pp 396-456.
- 21 5. Sobieski, L. A.; Tangney, T. J., Silicone Pressure Sensitive Adhesives. In *Handbook of*  
22 *pressure sensitive adhesives*, 2nd ed.; Satas, D., Ed. Van Nostrand Reinhold: New York,  
23 1989; Vol. 1, pp 508-526.
- 24 6. Lindner, A.; Lestriez, B.; Mariot, S.; Creton, C.; Maevis, T.; Luhmann, B.; Brummer,  
25 R. *Journal of Adhesion* **2006**, *82*, (3), 267-310.
- 26 7. Creton, C.; Hu, G. J.; Deplace, F.; Morgret, L.; Shull, K. R. *Macromolecules* **2009**, *42*,  
27 7605-7615.
- 28 8. Jovanovic, R.; Dubé, M. A. *Journal of Macromoleculaar Science Part C: Polymer*  
29 *Reviews* **2004**, *C44*, (1), 1-51.
- 30 9. Joanicot, M.; Wong, K.; Cabane, B. *Macromolecules* **1996**, *29*, 4976-4984.
- 31 10. Keddie, J. L. *Materials Science & Engineering R-Reports* **1997**, *21*, (3), 101-170.
- 32 11. Landfester, K. *Macromolecular Rapid Communications* **2001**, *22*, (12), 896-936.
- 33 12. Asua, J. M. *Progress in Polymer Science* **2002**, *27*, (7), 1283-1346.
- 34 13. El-Aasser, M. S.; Sudol, E. D. In *Miniemulsions: Overview of research and*  
35 *applications*, Roy W Tess Award in Coatings Symposium, Boston, MA, Aug, 2002; Boston,  
36 MA, 2002; pp 21-31.
- 37 14. Schork, F. J.; Luo, Y. W.; Smulders, W.; Russum, J. P.; Butte, A.; Fontenot, K.,  
38 Miniemulsion polymerization. In *Polymer Particles*, 2005; Vol. 175, pp 129-255.
- 39 15. Hegedus, C. R.; Kloiber, K. A. *Journal of Coatings Technology* **1996**, *68*, (860), 39-&.
- 40 16. Hirose, M.; Kadowaki, F.; Zhou, J. H. *Prog. Org. Coat.* **1997**, *31*, (1-2), 157-169.
- 41 17. Kukanja, D.; Golob, J.; Zupancic-Vlant, A.; Kranjc, M. *Journal of Applied Polymer*  
42 *Science* **2000**, *78*, 67-80.
- 43 18. Wang, C.; Chu, F.; Graillat, C.; Guyot, A. *Polymer Reaction Engineering* **2003**, *11*,  
44 (3), 541-562.
- 45 19. Wang, C.; Chu, F.; Graillat, C.; Guyot, A.; Gauthier, C. *Polymers For Advanced*  
46 *TEchnologies* **2005**, *16*, 139-145.
- 47 20. Wang, C.; Chu, F.; Graillat, C.; Guyot, A.; Gauthier, C.; Chapel, J. P. *Polymer* **2005**,  
48 *46*, 1113-1124.

- 1  
2 21. Wang, C.; Chu, F.; Guyot, A. *Journal of Dispersion Science and Technology* **2006**, 27,  
3 (3), 325-330.  
4 22. Wang, C. P.; Chu, F. X.; Jin, L. W.; Lin, M. T.; Xu, Y. Z.; Guyot, A. *Polymers For*  
5 *Advanced TEchnologies* **2009**, 20, (3), 319-326.  
6 23. Li, M.; Daniel, E. S.; Dimonie; Sudol, E. D.; El-Aasser, M. S. *Macromolecules* **2005**,  
7 38, 4183-4192.  
8 24. Hirose, M.; Zhou, J. H.; Nagai, K. *Prog. Org. Coat.* **2000**, 38, (1), 27-34.  
9 25. Sebenik, U.; Krajnc, M. *Journal of Polymer Science Part A: Polymer Chemistry* **2005**,  
10 43, 4050-4069.  
11 26. Deplace, F.; Rabjohns, M. A.; Yamaguchi, T.; Foster, A. B.; Carelli, C.; Lei, C. H.;  
12 Ouzineb, K.; Keddie, J. L.; Lovell, P. A.; Creton, C. *Soft Matter* **2009**, 5, 1440-1447.  
13 27. Zosel, A. *Colloid and Polymer Science* **1985**, 263, 541-553.  
14 28. Lakrout, H.; Sergot, P.; Creton, C. *Journal of Adhesion* **1999**, 69, (3/4), 307-359.  
15 29. Zosel, A. *Journal of Adhesion* **1989**, 30, (1-4), 135-149.  
16 30. Deplace, F.; Carelli, C.; Mariot, S.; Retsos, H.; Chateauminois, A.; Ouzineb, K.;  
17 Creton, C. *Journal of Adhesion* **2009**, 85, 18-54.  
18 31. Yamaguchi, T.; Koike, K.; Doi, M. *Epl* **2007**, 77, (6).  
19 32. Turreda, L. D.; Sonoda, H.; Hatano, Y.; Mizumachi, H. *Holzforschung* **1991**, 45, (6),  
20 461-466.  
21 33. Tse, M. F.; Jacob, L. *Journal of Adhesion* **1996**, 56, 79-95.  
22 34. Chang, E. P. *Journal of Adhesion* **1991**, 34, 189-200.  
23 35. Yang, H. W. H.; Chang, E. P. *Trends in Polymer Science* **1997**, 5, (11), 380-384.  
24 36. Creton, C.; Leibler, L. *Journal of Polymer Science Part B: Polymer physics* **1996**, 34,  
25 545-554.  
26 37. Carelli, C.; Deplace, F.; Boissonnet, L.; Creton, C. *Journal of Adhesion* **2007**.  
27 38. Nase, J.; Lindner, A.; Creton, C. *Physical Review Letters* **2008**, 101, 074503.  
28 39. Deplace, F. Adhésifs Nanostructurés en Voie Emulsion. University Paris VI, Paris,  
29 2008.  
30 40. Glassmaker, N. J.; Hui, C. Y.; Yamaguchi, T.; Creton, C. *European Physical Journal*  
31 *E* **2008**, 25, (3), 253-266.  
32 41. Good, R. J. *Journal of Adhesion* **1972**, 4, 133-154.  
33 42. Verdier, C.; Piau, J. M. *Journal of Polymer Science Part B-Polymer Physics* **2003**, 41,  
34 (23), 3139-3149.  
35 43. Roos, A.; Creton, C. *Macromolecules* **2005**, 38, (18), 7807-7818.  
36 44. Erk, K. A.; Henderson, K. J.; Shull, K. R. *Biomacromolecules* 11, (5), 1358-1363.  
37 45. Grassl, B.; Alb, A. M.; Reed, W. F. *Macromolecular Chemistry and Physics* **2001**,  
38 202, (12), 2518-2524.  
39 46. Lopez, A.; Degrandi, E.; Creton, C.; Asua, J. M., Simultaneous Free Radical and  
40 Addition Miniemulsion Polymerization: Effect of the Diol on the Microstructure of  
41 Polyurethane-Acrylic Pressure Sensitive Adhesives. submitted to *Polymer*, 2010.  
42 47. Florez, S.; Munoz, M. E.; Santamaria, A. *Macromolecules Materials Engineering*  
43 **2006**, 291, 1194-1200.  
44 48. Tong, J. D.; Jerome, R. *Polymer* **2000**, 41, (7), 2499-2510.  
45 49. Moghbeli, M. R.; Zamir, S. M.; Molaei, B. *Journal of Applied Polymer Science* **2008**,  
46 108, (1), 606-613.  
47 50. Wang, C.; Chu, F.; Guyot, A.; C., G.; F., B. *Journal of Applied Polymer Science* **2006**,  
48 101, 3927-3941.  
49 51. Bellamine, A.; Degrandi, E.; Gerst, M.; Stark, R.; Beyers, C.; Creton, C.  
50 *Macromolecular Materials and Engineering* **2010**, 295.

30

1  
2  
3  
4  
5  
6  
7  
8  
9  
10  
11  
12  
13  
14  
15  
16  
17  
18  
19  
20  
21  
22  
23  
24  
25  
26  
27  
28  
29  
30  
31  
32  
33  
34  
35  
36  
37  
38  
39  
40  
41  
42  
43  
44  
45  
46  
47  
48  
49  
50  
51  
52  
53  
54  
55  
56  
57  
58  
59  
60

For Review - Confidential - ACS